DR. GENEVIÈVE M NESSLAGE (Orcid ID : 0000-0003-1770-6803)

Article type : Original Article

Environmental drivers of golden tilefish (*Lopholatilus chamaeleonticeps*) commercial landings and catch-per-unit-effort

Geneviève Nesslage[1*], Vyacheslav Lyubchich[1], Paul Nitschke[2], Erik Williams[3], Churchill Grimes[4], and John Wiedenmann[5]

[1]Chesapeake Biological Laboratory, University of Maryland Center for Environmental Science, 146 Williams Street // 0038, Solomons, Maryland 20688, USA.

[2]National Oceanic and Atmospheric Administration, National Marine Fisheries Service, Northeast Fisheries Science Center, 166 Water St, Woods Hole, Massachusetts 02543, USA

[3]National Oceanic and Atmospheric Administration, National Marine Fisheries Service, Southeast Fisheries Science Center, Beaufort Laboratory, 101 Pivers Island Road, Beaufort, North Carolina 28516, USA

[4]National Oceanic and Atmospheric Administration, National Marine Fisheries Service, Retired, 211 Moriah Creek Road, Crawfordville, Florida 32327, USA

[5]Department of Ecology, Evolution, and Natural Resources, Rutgers University, New Brunswick, New Jersey 08901, USA

***Corresponding author:** Geneviève Nesslage, nesslage@umces.edu, 410-326-7223

Running title: Golden tilefish environmental drivers

ACKNOWLEDGEMENTS

This project was funded by the National Oceanic and Atmospheric Administration's Fisheries And The Environment program (NA14OAR4320158). We thank the two anonymous reviewers of our manuscript for their time and constructive comments. We also thank all those who provided data and advice for the project, including SCDNR's Marine Resources Monitoring Assessment and Prediction (MARMAP) program, Tracey Smart, Kevin McCarthy, and Harvey Walsh. Analyses and conclusions resulting from the use of MARMAP data are not necessarily those of the originating program. The Florida Current cable and section data are made freely available on the Atlantic Oceanographic and Meteorological Laboratory web page (www.aoml.noaa.gov/phod/floridacurrent/) and are funded by the DOC-NOAA Climate Program Office - Ocean Observing and Monitoring Division. The scientific results and conclusions, as well as any views or opinions expressed herein, are those of the authors and do not necessarily reflect those of NOAA or the Department of Commerce. This is contribution number XXXX of the University of Maryland Center for Environmental Science.

DATA AVAILABILITY

This article contains no new data. Environmental data sources used in this study are cited in the references section. Compiled commercial landings data and analysis R code are freely available on GitHub (https://github.com/vlyubchich/tilefish; Lyubchich & Nesslage, 2020). Commercial catch and effort data (source: National Marine Fisheries Service) used in this study are confidential at the spatiotemporal level analyzed and cannot be made publicly available.

ABSTRACT

We explored a range of potential low and high frequency environmental drivers of fishery production (landings) and catch-per-unit-effort (CPUE) for northern and southern stocks of golden tilefish (*Lopholatilus chamaeleonticeps*), a stenothermic species that prefers a narrow band of habitat along the continental shelf and upper slope of the eastern U.S. Random forest regression, a machine learning technique, was used to examine the impact of numerous and sometimes correlated environmental covariates. We used important random forest covariates to inform construction of a more parsimonious generalized additive mixed model for each data type and stock. We identified several potential environmental drivers of golden tilefish fishery and stock dynamics, including low frequency climate indices, oceanographic currents, and high frequency oceanographic conditions. Both Atlantic Multidecadal Oscillation (AMO) and North Atlantic Oscillation indices were associated with historical golden tilefish landings for the northern stock spanning 1915–2000 at lags of 7 and 3–4 years, respectively. CPUE for both stocks (north: 1995–2017, south: 1994–2018) was associated with the AMO and oceanographic currents. In addition, northern stock CPUE was negatively related to Labrador Current flow and positively related to northerly position of the Gulf Stream. Southern stock CPUE was associated with seasonal Florida Current transport, monthly sea surface temperatures, and latitude. Oceanographic currents and water temperature primarily influenced within-year CPUE, indicating a potential effect on adult fish or fisher behavior. In contrast, low frequency climate indices were associated with CPUE and landings at lags of 3–7 years, indicating their primary impact was on recruitment strength.

KEYWORDS

Golden tilefish, *Lopholatilus chamaeleonticeps*, environmental driver, random forest, machine learning, generalized additive model, mixed model

1. INTRODUCTION

Identifying environmental factors that drive fluctuations in fish catches and catch-per-unit-effort (CPUE) is one of the oldest goals of fisheries science (Smith, 1994). Continued interest in environmental influences is driven in part by a desire to improve stock assessment and provide more accurate advice for management. Understanding the relationship between ecosystem conditions and fishery production or CPUE has been shown, in certain circumstances, to enhance our ability to generate more accurate population hindcasts and forecasts for fisheries management (Fu et al., 2012; Fu et al., 2015; Gaichas, Bundy, Miller, Moksness, & Stergiou, 2012; Haltuch & Punt, 2011). Important environmental drivers of fishery processes include either high frequency (seasonal) conditions or low frequency (long-term) climate patterns and directional climate change (Hollowed et al., 2013; Tommasi, Stock, Hobday, et al., 2017; Tommasi, Stock, Pegion, et al., 2017). Although similar environmental drivers have been found to be influential across a range of species, key drivers are generally system-specific (Link et al., 2012).

Both low and high frequency environmental drivers have been hypothesized to impact the population dynamics and fishery catches of the northern and southern stocks of golden tilefish (*Lopholatilus chamaeleonticeps*) along the U.S. East Coast in the Northwest Atlantic (Figure 1; Barans & Stender, 1993; Grimes, Able, & Jones, 1986; Grimes, Able, & Turner, 1980; Marsh et al., 1999). Golden tilefish is thought to be particularly susceptible to environmental fluctuations given it is a stenothermic species that prefers a narrow band of habitat along the continental shelf and upper slope that is 9–14˚C and 80–305 m deep (Able, Grimes, Jones, & Twichell, 1993; Grimes et al., 1986; Grimes & Turner, 1999). In particular, the northern stock has been identified as being highly vulnerable to climate change (Hare et al., 2016). An example of the northern stock's potential susceptibility to environmental conditions was the 1882 die-off in which millions of golden tilefish died in a sudden and extensive mortality event (Bumpus, 1899; Collins, 1884). Marsh et al. (1999) suggested this die-off was the result of an extreme negative North Atlantic Oscillation (NAO) anomaly in 1881 that caused the intrusion of cold, subarctic water along the southern New England-Mid Atlantic shelf in the following year (Fisher, Frank, Petrie, & Leggett, 2014; Marsh et al., 1999). To address this hypothesis, Fisher et al. (2014) correlated historical northern landings of golden tilefish with the NAO and shelf slope water temperature anomalies and found a significant positive lagged correlation between landings and both the NAO (lags of 4–7 years) and bottom water temperature (lags of 3–4 years). However, this relationship broke down following development of the modern longline fishery in the mid-1970s, and Fisher et al. (2014) suggested that changes in fishing effort may have masked the detection of environmental impacts on tilefish landings as has been observed for other stocks (Drinkwater & Myers, 1987; Myers, 1998).

High frequency variation in bottom temperature along the Southern New England shelf has also been suggested as a driver of fishery dynamics for the northern golden tilefish stock. Seasonal cooling is thought to force tilefish to concentrate as the narrow band they inhabit along the upper continental shelf is reduced in spring (Grimes et al., 1986; Grimes et al., 1980). In the 1970s when the stock was relatively lightly exploited, fishers were known to target spring tilefish aggregations, producing relatively high CPUE that may not be proportional to overall abundance (Grimes et al., 1980). Such temperature-driven fisher behavior could be problematic for golden tilefish stock assessment. If CPUE is indicative of environmentally-driven changes in fisher success rather than abundance trends, the resulting fishery-dependent CPUE index will not be proportional to population abundance. In the absence of a long-term fishery-independent survey that reliably catches golden tilefish, both stock assessments rely exclusively (northern) or heavily (southern) on fishery-dependent CPUE trends as indices of abundance (Nesslage, 2016; Nitschke, 2017), making assessment results susceptible to bias if the impact of environmental drivers on fisher behavior affects the ability of the index to reflect trends in population abundance.

Less is known about environmental impacts on the southern stock of golden tilefish. Spawning females have been found at temperatures in the narrow band of 10.16–14.90°C off the Carolinas (Sedberry, Pashuk, Wyanski, Stephen, & Weinbach, 2006). Also, fishery-independent CPUE was found to increase across a temperature range of 9–15˚C in waters off South Carolina and Georgia (Barans & Stender, 1993; Low, Ulrich, & Blum, 1983). However, golden tilefish die-off events have not been observed in the southeastern U.S., and the extent to which climate fluctuations drive dynamics of the southern stock is unknown.

In this study, we comprehensively explored a range of potential low and high frequency environmental drivers of golden tilefish fishery production and CPUE for both the northern and southern stocks. Our objectives were to: 1) identify the best low frequency environmental predictors of golden tilefish landings, and 2) identify the primary environmental factors (both low and high frequency) related to golden tilefish CPUE.

2. METHODS

We used random forest regression (RF; Breiman, 2001; Hastie, Tibshirani, & Friedman, 2009) to explore a wide range of environmental factors that might explain long-term trends in golden tilefish landings and CPUE. RF allowed us to examine the impact of numerous and sometimes similar or correlated covariates. We then used the results of the RF to inform construction of a more parsimonious generalized additive mixed model (GAMM; S. Wood, 2006; Zuur, Ieno, Walker, Saveliev, & Smith, 2009). Environmental drivers of total historical landings were examined for the northern stock to expand directly upon the work of Fisher et al. (2014); the landings time series for the southern stock was too short to conduct a similar analysis. We also identified important environmental drivers of CPUE for both stocks to account for the impact of changes in fishery effort on landings trends (Harley, Myers, & Dunn, 2001; Pauly, Hilborn, & Branch, 2013). Compiled data and analysis R code are freely available on GitHub (https://github.com/vlyubchich/tilefish; Lyubchich & Nesslage, 2020) for the golden tilefish landings analysis. Commercial CPUE data used in this study are confidential at the spatiotemporal level analyzed and thus cannot be made publicly available.

2.1. Data sources

A time series of historical landings for the northern stock was constructed by summing commercial pounds landed annually across all gears from 1915 to 2017 (Nitschke, 2017). We did not include recreational data in this analysis because recreational removals are a very minor component of the overall catch and a reliable catch series could not be generated for the northern stock (NEFSC, 2014). Data from 2001–2017 were removed from the analysis to exclude the period in which landings were quota-limited. A comparably long time series of historical landings was not available for the southern stock given the fishery began in the mid-1970s (SEDAR, 2011).

CPUE for the northern stock was defined as pounds kept divided by days at sea (minus one day of steam time) using data collected from bottom longline Fishing Vessel Trip Reports spanning 1995–2017 (Nitschke, 2017). For the southern stock, CPUE was defined as gutted weight in pounds landed divided by days at sea using data collected from the bottom longline fishery's Coastal Fisheries Logbook Program spanning 1994–2018 (Nesslage, 2016). All CPUE data were aggregated on a monthly basis by National Marine Fisheries Service (NMFS) statistical area (Figure 1). We focused solely on analysis of longline sector CPUE data for three reasons: 1) longlines are the primary gear used in both northern and southern fisheries (mean >90% longline) during the extent of the available CPUE time series, and 2) the northern longline fishery is dedicated to tilefish and actively targets them, whereas most other commercial catch is bycatch in the trawl fishery, and 3) the southern handline fishery is quite small and does not have adequate data to construct a time series of CPUE (Nesslage, 2016).

Our exploratory analysis identified right skewness of the landings and CPUE data. To make the data distributions more symmetric and to satisfy the assumption of normality of residuals in GAMMs, we applied square root transformation to all response variables. For consistency and ease of comparison across modeling approaches, the transformed versions of the response variables were also used in the random forests.

Multiple data sources were used to generate environmental covariates in both landings and CPUE analyses, including long-term climate indices, indices of oceanic currents, and observed ocean conditions (Table 1). For both stocks, two low frequency climate indices were explored, namely the NAO and the Atlantic Multidecadal Oscillation (AMO; Delworth, Zhang, & Mann, 2007; Knight, Allan, Folland, Vellinga, & Mann, 2005), also known as Atlantic Multidecadal Variability. The NAO was a primary factor for consideration given previously demonstrated linkages between this index of sea level pressure in the North Atlantic and northern golden tilefish landings (Appenzeller, Stocker, & Anklin, 1998; Fisher et al., 2014; J. W. Hurrell & Deser, 2010). To determine which form of the NAO index is most relevant for golden tilefish, we considered four versions of the index spanning either December to February (Fisher et al., 2014) or December to April (Marsh et al., 1999) using both station- and principle component (PC)-based indices (J. Hurrell & National Center for Atmospheric Research Staff, 2020; National Center for Atmospheric Research Staff (Eds.), 2020). Station-based indices that extend back to the early 1900s were explored to mirror the northern stock landings analyses conducted by Fisher et al. (2014); however, more commonly used PC-based indices were explored in analyses of the recent time series of CPUE for both northern and southern stocks.

In addition to the NAO, we examined potential effects of the AMO, an index of detrended sea surface temperature (SST) anomalies averaged over the North Atlantic that is indicative of climate variability, based partially on the hypotheses of Marsh et al. (1999) and because many other species in the Northwest Atlantic have exhibited population fluctuations that are linked to broad-scale patterns in SST over time (Alheit et al., 2014; Auber, Travers-Trolet, Villanueva, & Ernande, 2015; Collie, Wood, & Jeffries, 2008). We considered annual AMO because this index had not been previously explored for tilefish as well as December to April AMO to span the time frame of NAO indices explored in previous tilefish studies (https://www.esrl.noaa.gov/psd/data/timeseries/AMO; Fisher et al., 2014; Marsh et al., 1999).

For analyses of CPUE in recent decades, a wider range of environmental data was available for inclusion in our analyses. First, we considered several metrics of oceanic currents as potential environmental drivers of CPUE (Table 1). Marsh et al. (1999) suggested that the 1882 golden tilefish die-off event was the result of a sudden southward expansion of cold water transport via the Labrador Current coincident with a large negative NAO anomaly in the previous year. Therefore, we obtained quarterly indices of Labrador Current surface (200 m) volume transport along four TOPEX/Poseidon-Jason tracks spanning 1992 to 2013 for consideration in northern stock analyses (DFO Canada, 2019; Han & Li, 2008). Given the possible influence of oceanic transport on golden tilefish dynamics, we also explored several indices of Gulf Stream position and flow for the northern stock, including annual anomalies in the Gulf Stream's position in the western North Atlantic (Northeast Fisheries Science Center, 2020) and both annual and quarterly indices of Gulf Stream transport and position of the Gulf Stream north wall (positive values represent a more northerly position; Watelet, 2019; Watelet, Beckers, & Barth, 2017). For the southern stock, we considered a monthly index of daily mean transport in the Florida Current, the southernmost portion of the Gulf Stream System (Atlantic Oceanographic and Meteorological Laboratory Physical Oceanography Division, 2019). Finally, because golden tilefish are a demersal species, we also considered an index of annual average bottom temperature anomalies in the Mid-Atlantic Bight generated from data collected on

Northeast Fisheries Science Center surveys, 1977–present (Northeast Fisheries Science Center, 2020), in the northern CPUE model.

High frequency environmental factors considered in our CPUE analyses were obtained from the International Comprehensive Ocean-Atmosphere Data Set (ICOADS; https://icoads.noaa.gov/) of surface marine products. Variables included SST and sea level pressure, vector wind northward and eastward components, and scalar wind. Data were averaged monthly across 1° latitude × 1° longitude boxes and assigned to the nearest NMFS statistical area. These data were included in our analyses in order to represent localized monthly sea conditions and capture the signature of seasonal and episodic phenomenon such as upwelling that may impact tilefish landings and CPUE. For the southern stock, bottom temperature data from South Carolina Department of Natural Resources' Marine Resources Monitoring, Assessment, and Prediction (MARMAP) longline survey were considered; however, the spatiotemporal resolution of the data were not sufficient to inform our model.

In addition to environmental data, all analyses included a time block categorical variable to account for major changes in fishery prosecution and management over time. For the northern stock landings analysis, five time blocks were defined: 1) 1915–1920, the initial US Fisheries Commission campaign to expand the northern golden tilefish fishery (Freeman & Turner, 1977); 2) 1921–1940, the early trawl fishery; 3) 1941–1945, overall cessation of the fishery during World War II; 4) 1946–1970, the post-WWII pre-modern fishery; and 5) 1971–2000, the modern longline fishery. For analysis of the shorter northern stock CPUE time series, two time blocks were defined: 1) 1995-2000, advent of the modern longline fishery, and 2) 2001-2017, longline fishery quota enacted thought the Mid-Atlantic Fishery Management Council's Tilefish Fishery Management Plan (NEFSC, 2014). For analysis of CPUE in the southern fishery, two time blocks were defined: 1) 1994–2005, early period of the South Atlantic Fishery Management Council's Snapper-Grouper Fishery Management Plan, and 2) 2006–2018, management period that included closures and quota reductions (SEDAR, 2011).

CPUE models also included covariates for month and location of each NMFS statistical area. We used data from areas with at least 30 CPUE records in the analyzed period. For the northern stock CPUE, there were only three areas with adequate records given the centralized nature of the fishery; hence, we used a categorical variable "Area" to distinguish those locations.

For the southern stock CPUE, there were 20 areas with adequate records, enabling us to use latitude and longitude of the area centroids to model spatial patterns.

In addition to examining the impact of covariates on landings or CPUE in the same year (lag 0), we also explored a range of time lags for each covariate based on whether the hypothesized influence on tilefish dynamics was high or low frequency (Table 1). Low frequency covariates hypothesized to have long-term impacts on tilefish dynamics (e.g., climate indices like NAO; Fisher et al. 2014) were lagged by up to 7 years, representing the high end of ages typically selected by the fishery (Nitschke, 2018) and, thus, the maximum time frame in which we might expect to observe an impact in the commercial fishery data. We selected a shorter range of up to 3 years (i.e., time frame prior to age at first selection in fishery) for quarterly and monthly covariates representing hypothesized high frequency or short-term influences such as the Labrador Current and Gulf Stream indices. Covariates representing localized, short-term water conditions (e.g., monthly temperature, pressure, and wind metrics for each statistical area) were not lagged. Lagged covariates are indicated by the addition of parentheses "(t – X y/q/m)" with X representing the number of years, quarters, or months lagged, respectively.

2.2. Identifying environmental drivers using random forest regression

We used RF as the first step in variable selection and modeling (Breiman, 2001). To quantify uncertainty in the importance measure and describe the relative importance of a specific variable, we used two algorithms, Boruta (Kursa & Rudnicki, 2010) and Altmann et al. (2010), which have been shown to perform well in a variety of settings with correlated predictors (Degenhardt, Seifert, & Szymczak, 2019). Considering the large number of environmental covariates in our analysis, including their lagged versions, we treated environmental drivers as important only if they were selected by both Boruta and Altmann's algorithms. For more details on RF construction, see Supplementary Materials.

2.3. Statistical modeling of impact of environmental drivers on landings and CPUE

We used generalized additive models (GAMs) to generate more parsimonious statistical models of tilefish landings and CPUE. We used generalized additive models (GAMs) to generate more parsimonious statistical models of tilefish landings and CPUE. Given a GAM with too many explanatory variables may be impractical or even numerically impossible (Section 5.7; S. Wood, 2006; Zuur et al., 2009), a forward selection of relevant variables was implemented. One can add variables into a GAM based on their correlation with the response variable (strongest correlations first), but commonly used correlation coefficients measure strength of only linear (Pearson correlation coefficient) or monotonic (Spearman correlation coefficient) relationships, while GAMs allow us to model nonlinear and possibly nonmonotonic relationships, which would not be captured by Pearson or Spearman correlation. To match the GAM's purpose of handling nonlinear relationships, we used preliminary estimates and particularly importance rankings of such relationships obtained from our RFs. RF estimates nonlinear relationships that can be modeled also with GAMs, and variable importance in an RF is similar to the variance decomposition method LMG (named after the authors Lindeman, Merenda, & and Gold, 1980; Grömping, 2015). LMG is used in statistical regression modeling and satisfies more requirements for relative importance metrics than pairwise correlations, magnitude of regression coefficients, or their t-statistics (Grömping, 2015). Hence, we leveraged variable importance information from random forests, an approach that has been shown to perform well in a variety of studies with large number of predictors (Genuer, Poggi, & Tuleau-Malot, 2010; Hapfelmeier & Ulm, 2013; Oldekop, Holmes, Harris, & Evans, 2016; Sandri & Zuccolotto, 2006). Our RF contained many more variables than were retained in the GAMs (Table 1); therefore, the RF-based rankings allowed us to prioritize the examination of variables in a GAM, but did not restrict the selection pool considerably.

We assessed the contribution of each variable in the final GAM using the Shapley–Owen decomposition (Hüttner & Sunder, 2011) of the GAM's coefficient of determination (R^2). The decomposition determines how much an addition of each variable improves the final R^2. Since regressors are usually not perfectly independent, the calculations are repeated for all combinations of regressors x_j ($j = 1, \ldots, p$) in the model:

$$R_j^2 = \sum_{T \subseteq Z \setminus \{x_j\}} \frac{k!(p-k-1)!}{p!} \left[R^2(T \cup \{x_j\}) - R^2(T) \right], \tag{310}$$

where T is model with k regressors ($k = 0, \ldots, p - 1$); $T \cup \{x_j\}$ is the same model with regressor x_j included; Z is the set of all models with all combinations of regressors. We represent R_j^2 as percentage of the final GAM's R^2.

2.4. Model assessment

We compared GAMM and RF models by assessing their predictive performance on a testing set, using known values of the predictors in the testing set. We assumed that better predictive performance (lower prediction error) corresponds with better ability of the model to capture underlying relationships between the fishery data and environmental covariates.

For both southern and northern CPUE datasets, we used the training set extending up to 2010 to select predictors and estimate model parameters, then generated forecasts for 2011 and beyond (i.e., the testing set). To compare true data in the testing set with forecasts, we calculated and compared prediction mean absolute error (PMAE) and prediction root mean square error (PRMSE). Let $\hat{y}_i$ be the forecast values in the testing set of size n, and y_i be the corresponding real values, then

$$PMAE = n^{-1} \sum_{i=1}^{n} |y_i - \hat{y}_i|$$

$$PRMSE = \sqrt{n^{-1} \sum_{i=1}^{n} (y_i - \hat{y}_i)^2}$$

PMAE scores the forecast errors linearly, using the absolute values. PRMSE squares the errors before averaging; hence, PMAE and PRMSE are similar when variance in errors is small, but PRMSE is more sensitive and can better detect error outliers. Low prediction errors correspond to more accurate forecasts. The variable selection and model estimation process was repeated on the full dataset to obtain final models.

Several aspects of the northern tilefish landings dataset restricted us from implementing the same model validation scheme as for CPUE. First, the landings dataset was relatively small; therefore, we used the whole dataset in the variable selection process to capture the impact of low-frequency covariates on the landings. Second, because this longer dataset included distinct time blocks represented by a categorical variable, we modified the validation routine to ensure that a given time block was represented in both training and testing sets, and that the temporal order was preserved using the methods described in Supplementary Materials.

Within the outlined validation schemes, we obtained two types of forecasts from GAMMs: from the GAM part only by setting the random effects to zero, and from the full GAMM by additionally forecasting the AR(1) errors. For the latter type of forecasts, the last observed error is needed to calculate each new forecast; hence, such forecasts are essentially short-term, one-step-ahead, forecasts and their quality can be expected to be higher than that of GAMs.

3. RESULTS

We found that northern landings and CPUE models differed with respect to the significant covariates identified by RF regression models and GAMMs (Table 1). In addition, CPUE models generated for the northern stock included a different set of covariates from models generated for the southern stock. Given these differences, results are reported by dependent variable (landings and CPUE) and stock region (northern and southern). Final RF and GAMM model descriptions are provided below; additional modeling result details can be found in Supplementary Materials.

3.1. Northern stock landings

From the original 49 explanatory variables, the final RF model included 10 variables: annual AMO (lagged 5–7 years); December to April AMO (lagged 5–7 years); station-based December to February NAO (lagged 3 and 4 years); PC-based December to February NAO (lagged 4 years), and management time block (Table 1; Figure S3). The final GAMM based on backward selection of variables included December to April AMO lagged 7 years and station-based December to February NAO lagged 3 and 4 years (Table 1). The shapes of the relationships approximated by the RF and GAMM indicate that golden tilefish landings were higher during negative AMO and positive NAO, with their respective lags (Figures 2 and 3). The largest range of the smoothed term on the y-axis corresponded with December to April AMO lagged 7 years (Figures 2 and 3) and this covariate contributed 52.5% of the GAM R^2 (Figure 4), implying AMO has the largest influence on northern landings. In contrast, NAO covariates at lags of 3 and 4 years contributed a combined 47.5% of the GAM R^2 (Figure 4).

3.2. Northern stock CPUE

The random forest using the full dataset identified 62 significant variables from the original 121 explanatory variables (Table 1), including two versions of the AMO (annual and seasonal with each lagged 0–7 years), both seasonal versions of PC-based NAO (each lagged 0–7 years), Labrador Current transport indices (NE Track 191: lagged 0, 4, 9, and 10 quarters), Gulf Stream index of position anomalies (lagged 0, 1, 4–10, and 12 quarters), Gulf stream position indices (lagged 0–3 years), Gulf stream transport index (lagged 0–3 years), bottom temperature anomalies (lagged 0–2, 4–7 years), and time block (Figure S1). The final GAMM for northern CPUE included four variables: annual AMO lagged 6 years, December to April AMO lagged 7 years, Gulf Stream index of position anomalies lagged 12 quarters, and the Labrador Current transport index for NE Track 191 unlagged (Table 1; Figure 5). Annual AMO lagged 6 years and December to April AMO lagged 7 years contributed a combined 64.1% of the GAM R^2 (Figure 4). Gulf Stream and Labrador Current transport indices contributed only 19.7% and 16.2%, respectively, of the GAM R^2 (Figure 4).

3.3. Southern stock CPUE

The RF generated using the full dataset selected 53 out of 54 variables as important (only December to February NAO lagged 7 years was deemed unimportant; Figure S2). The final GAMM included 11 variables: time block; December to April AMO lagged 7 years; annual AMO lagged 2 and 4 years; Florida Current transport index lagged 2, 3, 4, 7, and 11 months; average monthly SST, and latitude (Table 1, Figure 6). The marginal contributions to the GAM R^2 were spread across a mixture of covariates, namely management time block (23.6%), December to April AMO lagged 7 years (17.6%), latitude (14.3%), annual AMO lagged 2 and 4 years (14.2%, 13.8%), Florida Current transport index (combined 14.5% across all lags), and SST (2%; Figure 4).

3.4. Model performance evaluation

The evaluation of predictive performance between RF and GAMMs demonstrated that the more parsimonious GAMMs were able to capture relationships between landings and environmental covariates better than RF (Table 2). This may be explained by the small size of the dataset and tendency of RF to over fit the data (Section 15.3.4 in Hastie et al. 2009). RF prediction errors for northern CPUE were smaller than of the GAM(M)s, but not substantially smaller compared to how many more variables were used in the RF. For southern CPUE, the GAMM was able to outperform RF by producing lower prediction errors.

4. DISCUSSION

We identified several potential environmental drivers of golden tilefish fishery and stock dynamics, including low frequency climate indices (AMO and NAO), oceanographic currents (Labrador and Florida Currents and the Gulf Stream), and high frequency oceanographic conditions (monthly sea surface temperature; Figures 2–5). Similar to Fisher et al. (2014), we identified a positive, lagged association between historical northern golden tilefish landings and the NAO (Figures 2–3). Our landings analysis differed from that of Fisher et al. (2014) in that we considered also the AMO, another potentially influential climate indicator. Over the time series of landings analyzed (1915–2000), we found the AMO with a lag of 7 years to be more influential than the NAO (Figures 3, S3, and 4a). While it is likely that the NAO, in concert with the Labrador Current, played a role in the 1882 die off as indicated in previous studies (Marsh et al., 1999), golden tilefish landings do not appear to be responding solely to NAO anomalies (Fisher et al., 2014). Complicating the relationship may be the influence of the AMO which has been linked to SST and precipitation fluctuations in a unique and complicated manner along the East Coast of the U.S. (Alexander, Kilbourne, & Nye, 2014) and associated with population dynamics of several Northwest Atlantic fishes (Buchheister et al., 2016; Midway et al., 2020; Nye et al., 2014).

Given golden tilefish recruit to the fishery around ages 4–5 years (Nesslage, 2016; Nitschke, 2017), our observed lagged relationships between landings and climate indices suggest the environment is impacting recruitment rather than adult survival or fisher behavior. Our findings add to the body of evidence suggesting the AMO has been a bottom-up driver of fish recruitment dynamics (Nye et al., 2014). However, AMO and NAO climate cycles are likely working together in a complex way to influence golden tilefish recruitment and subsequent fishery landings 3–7 years later. Climate variability patterns such as the NAO and AMO often interact, making it difficult to discern the individual effect of each climate index (Nye et al., 2014). The AMO has been shown to influence both primary production (Martinez, Antoine, D'Ortenzio, & Gentili, 2009) and ocean conditions, including winds and currents (Häkkinen, Rhines, & Worthen, 2011) and storm intensity (Schofield et al., 2008). The significant influence of AMO on tilefish recruitment indicated by our study would suggest the underlying mechanism may be AMO-induced fluctuations in primary production and/or impacts on larval transport as has been suggested for other fishes (Buchheister et al., 2016; Midway et al., 2020; R. J. Wood & Austin, 2009).

We found environmental factors associated with historical landings differed from that of CPUE. Given the much longer time series of landings relative to the availability of oceanographic data in both regions, the only covariates common to both landings and CPUE models were the climate indices. AMO was identified as an influential factor associated with both northern and southern CPUE, but the NAO was not included in the final, forward-selected GAMMs of CPUE for either stock, indicating the AMO is a more influential driver of CPUE (Figures 4b and 4c). In the north, CPUE was positively associated with the AMO at lags of 6–7 years in a largely linear fashion (Figure 5). Southern stock CPUE was positively associated with the AMO with a similar lag of 7 years, but also at lags of 2 and 4 years and in a more non-linear fashion (Figure 6). Whereas the AMO was negatively associated with northern landings 7 years later, the AMO was positively associated with both northern CPUE (lags 6–7 years) and southern CPUE (lags 2, 4, and 7 years). This discrepancy was likely due to the difference in time series length between the northern landings model (86 years) and the northern and southern CPUE models (23 and 24 years, respectively). The longer time series of landings included a wider range of AMO-associated climate variability as demonstrated by the wider range of x-axis values in Figures 3 vs Figures 5 and 6. Also, inclusion of early (pre-longline) fisheries in the historical landings time series could have influenced model results if AMO-driven shifts in target species or areas fished differed among current and historical fleets; similarly, the northern CPUE time series included the quota managed time block, which was excluded from the landings time series analysis.

In addition to the AMO, oceanographic currents were found to be associated with both northern and southern stock CPUE. Southern stock CPUE was associated with seasonal Florida Current transport, but the direction of that relationship depended on the monthly lag (Figure 6). Northern stock CPUE was positively related to low Labrador Current flow in the same quarter and positive anomalies in Gulf Stream position (GSI) at a lag of 3 years (Figure 5), conditions in which cold water intrusion into golden tilefish habitat would be minimal (Northeast Fisheries Science Center, 2020). This general relationship between CPUE and northeastern oceanographic currents was hypothesized by Marsh et al. (1999) in their proposed explanation of the 1882 die-off event. Since the late 1950s, the position of the northern edge of the Gulf Stream has been moving northward and the rate of movement has been increasing since 2009 (Northeast Fisheries Science Center, 2020). If global climate change continues to affect oceanographic currents and circulation patterns, golden tilefish in the northern stock unit may exhibit a range shift into the Gulf of Maine in response to northerly movement of the Gulf Stream wall and warming ocean temperatures (Nye et al., 2014). It is not clear how long golden tilefish have been present in the Gulf of Maine, but novel catches in a recently developed cooperative Gulf of Maine bottom longline survey and occasional commercial catches suggest golden tilefish are present to some degree in isolated locations within the Gulf of Maine (NEFSC, 2019).

It is also worth noting that several oceanographic current covariates in our CPUE models were lagged seasonally, indicating that fish or fisher behavior may be influenced by oceanographic conditions (Figures 5-6). Overall, though, CPUE for both stocks was primarily influenced by covariates that were lagged across multiple years (Figure 4). This suggests that the environment is primarily affecting current recruitment and that its influence on catchability is unlikely to be causing a decoupling of northern and southern longline CPUE indices from stock trends.

The southern stock also displayed a strong association with localized monthly SST (Figure 6). Southern CPUE increased with decreasing SST, possibly indicating the potential positive impact on stock and fishery performance of upwelling events which are driven by the intrusion of cold water. Alternatively, CPUE may be high when SST is low because observations in the CPUE time series span a range of temperatures (Figure 6) that, near the sea floor, are likely approaching the upper range of golden tilefish's stenothermic temperature preferences (9–14˚C; Figure S4). A similar decline in CPUE at temperatures >14˚C was observed in fishery-independent surveys conducted in southern waters off South Carolina and Georgia (Barans & Stender, 1993; Low et al., 1983). We also found that southern stock CPUE increased at latitudes south of Cape Canaveral, Florida (approximately 28.4˚N; Figure 6), likely due to more suitable bottom temperatures observed at lower latitudes at depths golden tilefish typically inhabit (80–300m; Figure S4). In our study, SST was negatively associated with CPUE in the same month, which suggests immediate effects of water temperature on behavior and survival of adult fish or fisher behavior; however, the overall impact of temperature on CPUE index catchability is likely low given the SST covariate only contributed 2% of the GAM R^2 (Figure 4).

Although previous studies identified a seasonal pattern in golden tilefish CPUE for the northern stock (Grimes et al., 1980), we did not find strong evidence for an association between monthly northern CPUE and SST in this study. The lack of association between CPUE and SST may be explained by a decoupling between surface temperature and temperature near the sea floor where adult tilefish are found. Alternatively, latitudinal and temperature effects on CPUE may not have been as evident in the northern stock because the stock is concentrated in a relatively small number of NMFS statistical areas that do not span as wide a geographic area as the southern stock (Figure 1; Nitschke, 2017). In general, CPUE data available for use in this study were limited in spatiotemporal resolution to monthly reporting at the NMFS statistical area level, which may have affected our ability to identify other potential high frequency ocean condition drivers for both stocks. In addition, previous studies linking water temperature and seasonal CPUE (Grimes et al., 1980) were conducted in the 1970s when the northern stock was lightly exploited such that the effect of colder seasonal temperatures may have resulted in a larger overall population effect than in recent decades. Another complicating factor is increased and prolonged presence of spiny dogfish (*Squalus acanthias*) in golden tilefish habitat in recent decades during the winter and spring has led to lower golden tilefish catches and increased effort by fishers in an effort to avoid dogfish concentrations, a development that further complicates interpretation of abiotic environmental effects at small spatiotemporal scales in the north (MAFMC, 2020). Finally, increasing bottom temperatures due to climate change (Northeast Fisheries Science Center, 2020) may have lessened the observed influence of water temperatures on northern tilefish CPUE in recent years.

Although oceanographic currents and ocean conditions were associated with golden tilefish CPUE at a monthly to annual time scale, climate indices (AMO and NAO) appeared to be associated with stock (CPUE) and fishery (landings) dynamics at longer lags of 3-7 years, indicating their primary impact was on recruitment strength as opposed to within-year adult survival or fisher behavior. Climate conditions could be influencing golden tilefish larval transport and settlement success or quality of juvenile habitat. Cyclical patterns in estimated recruitment have been observed in both stock assessments with more pronounced regularity in the north, indicating environmental influences on stock productivity (Figure S5). However, almost nothing is known about the early life stages of this species because current ichthyoplankton surveys on the U.S. East Coast do not encounter golden tilefish frequently enough to inform trends in larval and juvenile tilefish for either stock (pers. comm. Harvey Walsh). Stakeholders, managers, and scientists are keenly interested in identifying the mechanism behind these recruitment cycles that sustain the golden tilefish fishery. Based on the high accuracy of some of our CPUE models and their efficient use of leading indicators (lagged covariates that can be used to predict CPUE several time steps in the future, without the need to forecast the covariates themselves), our study shows promise for development of predictive models of tilefish stock dynamics. This study lays the groundwork for future research on early life history of golden tilefish and improved methods for better incorporating recruitment uncertainty in stock assessment projections used in management.

CONFLICT OF INTEREST

None.

AUTHOR CONTRIBUTION

All authors contributed extensively to the work presented in this paper. All authors were active in designing the study, analyzing the data, interpreting the results, and writing the paper.

REFERENCES

Able, K., Grimes, C., Jones, R. S., & Twichell, D. C. (1993). Temporal and spatial variation in habitat characteristics of tilefish (*Lopholatilus chamaeleonticeps*) off the east coast of Florida. *Bulletin of Marine Science, 53*(3), 1013-1026.

Alexander, M. A., Kilbourne, K. H., & Nye, J. A. (2014). Climate variability during warm and cold phases of the Atlantic Multidecadal Oscillation (AMO) 1871–2008. *Journal of Marine Systems, 133*, 14-26.

Alheit, J., Licandro, P., Coombs, S., Garcia, A., Giráldez, A., Santamaría, M. T. G., . . . Tsikliras, A. C. (2014). Atlantic Multidecadal Oscillation (AMO) modulates dynamics of small pelagic fishes and ecosystem regime shifts in the eastern North and Central Atlantic. *Journal of Marine Systems, 133*, 88-102. doi: https://doi.org/10.1016/j.jmarsys.2014.02.005

Altmann, A., Toloşi, L., Sander, O., & Lengauer, T. (2010). Permutation importance: a corrected feature importance measure. *Bioinformatics, 26*(10), 1340-1347.

Appenzeller, C., Stocker, T., & Anklin, M. (1998). North Atlantic Oscillation dynamics recorded in Greenland ice cores. *Science, 282*(5388), 446-449.

Atlantic Oceanographic and Meteorological Laboratory Physical Oceanography Division. (2019). from https://www.aoml.noaa.gov/phod/floridacurrent/data_access.php

Auber, A., Travers-Trolet, M., Villanueva, M. C., & Ernande, B. (2015). Regime shift in an exploited fish community related to natural climate oscillations. *PloS One, 10*(7).

Barans, C. A., & Stender, B. W. (1993). Trends in tilefish distribution and relative abundance off South Carolina and Georgia. *Transactions of the American Fisheries Society, 122*(2), 165-178.

Breiman, L. (2001). Random forests. *Machine learning, 45*(1), 5-32.

Buchheister, A., Miller, T. J., Houde, E. D., Secor, D. H., & Latour, R. J. (2016). Spatial and temporal dynamics of Atlantic menhaden (*Brevoortia tyrannus*) recruitment in the Northwest Atlantic Ocean. *ICES Journal of Marine Science, 73*(4), 1147-1159. doi: 10.1093/icesjms/fsv260

Bumpus, H. (1899). On the reappearance of the Tile-Fish (*Lopholatilus chamealeonticeps*). *Science, 8*(200), 576-578.

Collie, J. S., Wood, A. D., & Jeffries, H. P. (2008). Long-term shifts in the species composition of a coastal fish community. *Canadian Journal of Fisheries and Aquatic Sciences, 65*(7), 1352-1365.

Collins, J. (1884). *History of the Tile-fish. Report of the Commissioner for 1882. U.S. Comm. Fish Fish., Pt. 10,* . Washington, D.C.

Degenhardt, F., Seifert, S., & Szymczak, S. (2019). Evaluation of variable selection methods for random forests and omics data sets. *Briefings in bioinformatics, 20*(2), 492-503.

Delworth, T. L., Zhang, R., & Mann, M. E. (2007). Decadal to centennial variability of the Atlantic from observations and models. *Geophysical Monograph-American Geophysical Union, 173*, 131.

DFO Canada. (2019). Atlantic Zone Monitoring Program. from http://www.dfo-mpo.gc.ca/science/data-donnees/azmp-pmza/index-eng.html

Drinkwater, K. F., & Myers, R. (1987). Testing predictions of marine fish and shellfish landings from environmental variables. *Canadian Journal of Fisheries and Aquatic Sciences, 44*(9), 1568-1573.

Fisher, J. A. D., Frank, K. T., Petrie, B., & Leggett, W. C. (2014). Life on the edge: environmental determinants of tilefish (*Lopholatilus chamaeleonticeps*) abundance since its virtual extinction in 1882. *ICES Journal of Marine Science: Journal du Conseil*. doi: 10.1093/icesjms/fsu053

Freeman, B. L., & Turner, S. C. (1977). *Biological and fisheries data on tilefish, Lopholatilus chamaeleonticeps Goode and Bean*. Sandy Hook Laboratory, Northeast Fisheries Center, National Marine Fisheries Service.

Fu, C., Gaichas, S., Link, J. S., Bundy, A., Boldt, J. L., Cook, A. M., . . . Friedland, K. D. (2012). Relative importance of fisheries, trophodynamic and environmental drivers in a series of marine ecosystems. *Marine Ecology Progress Series, 459*, 169-184.

Fu, C., Large, S., Knight, B., Richardson, A. J., Bundy, A., Reygondeau, G., . . . Sobrino, I. (2015). Relationships among fisheries exploitation, environmental conditions, and ecological indicators across a series of marine ecosystems. *Journal of Marine Systems, 148*, 101-111.

Gaichas, S. K., Bundy, A., Miller, T. J., Moksness, E., & Stergiou, K. I. (2012). What drives marine fisheries production? *Marine Ecology Progress Series, 459*, 159-163.

Genuer, R., Poggi, J., & Tuleau-Malot, C. (2010). Variable selection using random forests. *Pattern Recognition Letters, 31*(14), 2225-2236.

Grimes, C., Able, K., & Jones, R. S. (1986). Tilefish, *Lopholatilus chamaeleonticeps*, habitat, behavior and community structure in Mid-Atlantic and southern New England waters. *Environmental Biology of Fishes, 15*(4), 273-292.

Grimes, C., Able, K., & Turner, S. (1980). A preliminary analysis of the tilefish, *Lopholatilus chamaeleonticeps*, fishery in the Mid-Atlantic Bight. *Mar. Fish. Rev, 42*(11), 13-18.

Grimes, C., & Turner, S. (1999). The complex life history of tilefish *Lopholatilus chamaeleonticeps* and vulnerability to exploitation. *American Fisheries Society Symposium, 23*, 17-26.

Grömping, U. (2015). Variable importance in regression models. *WIREs Computational Statistics, 7*, 137-152.

Häkkinen, S., Rhines, P. B., & Worthen, D. L. (2011). Atmospheric blocking and Atlantic multidecadal ocean variability. *Science, 334*(6056), 655-659.

Haltuch, M. A., & Punt, A. E. (2011). The promises and pitfalls of including decadal-scale climate forcing of recruitment in groundfish stock assessment. *Canadian Journal of Fisheries and Aquatic Sciences, 68*(5), 912-926.

Han, G., & Li, J. (2008). Sea level and geostrophic current features from tandem TOPEX/Poseidon-Jason data in the Newfoundland offshore. *International Journal of Remote Sensing, 29*(1), 265-280.

Hapfelmeier, A., & Ulm, K. (2013). A new variable selection approach using random forests. *Computational Statistics & Data Analysis, 60*, 50-69.

Hare, J. A., Morrison, W. E., Nelson, M. W., Stachura, M. M., Teeters, E. J., Griffis, R. B., . . . Bell, R. J. (2016). A vulnerability assessment of fish and invertebrates to climate change on the Northeast US Continental Shelf. *PloS One, 11*(2), e0146756.

Harley, S. J., Myers, R. A., & Dunn, A. (2001). Is catch-per-unit-effort proportional to abundance? *Canadian Journal of Fisheries and Aquatic Sciences, 58*(9), 1760-1772.

Hastie, T., Tibshirani, R., & Friedman, J. (2009). *The elements of statistical learning: data mining, inference, and prediction*: Springer Science & Business Media.

Hollowed, A. B., Barange, M., Beamish, R. J., Brander, K., Cochrane, K., Drinkwater, K., . . . Ito, S. (2013). Projected impacts of climate change on marine fish and fisheries. *ICES Journal of Marine Science, 70*(5), 1023-1037.

Hurrell, J., & National Center for Atmospheric Research Staff. (2020). The Climate Data Guide: Hurrell North Atlantic Oscillation (NAO) Index (station-based). Accessed 5/11/2017. from https://climatedataguide.ucar.edu/climate-data/hurrell-north-atlantic-oscillation-nao-index-station-based

Hurrell, J. W., & Deser, C. (2010). North Atlantic climate variability: the role of the North Atlantic Oscillation. *Journal of Marine Systems, 79*(3), 231-244.
Hüttner, F., & Sunder, M. (2011). Decomposing R2 with the Owen value. *Working Papers from University of Leipzig, Faculty of Economics and Management Science. No 100*.
Knight, J. R., Allan, R. J., Folland, C. K., Vellinga, M., & Mann, M. E. (2005). A signature of persistent natural thermohaline circulation cycles in observed climate. *Geophysical Research Letters, 32*(20).
Kursa, M. B., & Rudnicki, W. R. (2010). Feature selection with the Boruta package. *Journal of Statistical Software, 36*(11), 1-13.
Lindeman, R., Merenda, P., & and Gold, R. (1980). *Introduction to Bivariate and Multivariate Analysis, Glenview, IL: Scott, Foresman.*
Link, J. S., Gaichas, S., Miller, T. J., Essington, T., Bundy, A., Boldt, J., . . . Moksness, E. (2012). Synthesizing lessons learned from comparing fisheries production in 13 northern hemisphere ecosystems: emergent fundamental features. *Marine Ecology Progress Series, 459*, 293-302.
Low, R., Ulrich, G., & Blum, F. (1983). Tilefish off South Carolina and Georgia. *Marine Fisheries Review, 45*(4-6), 16-26.
Lyubchich, V., & Nesslage, G. (2020). *Environmental Drivers of Golden Tilefish Landings v1.0*: Zenodo. DOI: 10.5281/zenodo.3732839.
MAFMC. (2020). Golden Tilefish Fishery Performance Report. from https://static1.squarespace.com/static/511cdc7fe4b00307a2628ac6/t/5e56900f0e338c4b795be8d4/1582731279530/2020_GTF_FPR_Final.pdf
Marsh, R., Petrie, B., Weidman, C. R., Dickson, R. R., Loder, J. W., Hannah, C. G., . . . Drinkwater, K. (1999). The 1882 tilefish kill—a cold event in shelf waters off the north-eastern United States? *Fisheries Oceanography, 8*(1), 39-49.
Martinez, E., Antoine, D., D'Ortenzio, F., & Gentili, B. (2009). Climate-driven basin-scale decadal oscillations of oceanic phytoplankton. *Science, 326*(5957), 1253-1256.
Midway, S. R., Schueller, A. M., Leaf, R. T., Nesslage, G. M., & Mroch III, R. M. (2020). Macroscale drivers of Atlantic and Gulf Menhaden growth. *Fisheries Oceanography, 29*(3), 252-264. doi: 10.1111/fog.12468

Myers, R. A. (1998). When do environment–recruitment correlations work? *Reviews in Fish Biology and Fisheries, 8*(3), 285-305.

National Center for Atmospheric Research Staff (Eds.). (2020). The Climate Data Guide: Hurrell North Atlantic Oscillation (NAO) Index (PC-based). Accessed 5/11/2017. from https://climatedataguide.ucar.edu/climate-data/hurrell-north-atlantic-oscillation-nao-index-pc-based

NEFSC. (2014). 58th Northeast Regional Stock Assessment Workshop (58th SAW) Assessment Report. US Dept Commer, Northeast Fish Sci Cent Ref Doc. 14-04; 784 p.

NEFSC. (2019). Design, Implementation, and Results of a Cooperative Research Gulf of Maine Longline Survey, 2014-2017. NOAA technical memorandum NMFS-NE ; 249. doi: https://doi.org/10.25923/2sgn-mx62

Nesslage, G. (2016). Stock Assessment of Golden Tilefish off the Southeastern United States: 2016 SEDAR Update Assessment. SEFSC, Beaufort Laboratory, Beaufort, NC.

Nitschke, P. (2017). Golden Tilefish, *Lopholatilus chamaeleonticeps*, stock assessment update through 2016 in the Middle Atlantic-Southern New England Region. National Marine Fisheries Service, Northeast Fisheries Science Center, Woods Hole, MA.

Nitschke, P. (2018). Golden Tilefish, *Lopholatilus chamaeleonticeps*, data update through 2017 in the Middle Atlantic-Southern New England Region. Northeast Fisheries Science Center, Woods Hole, MA.

Northeast Fisheries Science Center. (2020). Technical Documentation, State of the Ecosystem Report. https://noaa-edab.github.io/tech-doc/

Nye, J. A., Baker, M. R., Bell, R., Kenny, A., Kilbourne, K. H., Friedland, K. D., . . . Wood, R. (2014). Ecosystem effects of the atlantic multidecadal oscillation. *Journal of Marine Systems, 133*, 103-116.

Oldekop, J., Holmes, G., Harris, W., & Evans, K. (2016). A global assessment of the social and conservation outcomes of protected areas. *Conservation Biology in Practice, 30*(1), 133-141.

Pauly, D., Hilborn, R., & Branch, T. A. (2013). Fisheries: Does catch reflect abundance? *Nature, 494*(7437), 303.

Sandri, M., & Zuccolotto, P. (2006). Variable Selection Using Random Forests. In S. Zani, A. Cerioli, M. Riani & M. Vichi (Eds.), *Data Analysis, Classification and the Forward*

Search. Studies in Classification, Data Analysis, and Knowledge Organization. Berlin, Heidelberg: Springer.

Schofield, O., Chant, R., Cahill, B., Castelao, R., Gong, D., Kahl, A., . . . Ramey, P. (2008). The decadal view of the Mid-Atlantic Bight from the COOLroom: Is our coastal system changing? *Oceanography, 21*(4), 108-117.

SEDAR. (2011). SEDAR 25 – South Atlantic Tilefish Stock Assessment Report. North Charleston, SC. Available online at: http://sedarweb.org/sedar-25.

Sedberry, G., Pashuk, O., Wyanski, D., Stephen, J., & Weinbach, P. (2006). Spawning locations for Atlantic reef fishes off the southeastern US. *Proceedings of the Gulf and Caribbean Fisheries Institute, 57*, 463-514.

Smith, T. D. (1994). *Scaling fisheries: the science of measuring the effects of fishing, 1855-1955*: Cambridge University Press.

Tommasi, D., Stock, C. A., Hobday, A. J., Methot, R., Kaplan, I. C., Eveson, J. P., . . . Gehlen, M. (2017). Managing living marine resources in a dynamic environment: the role of seasonal to decadal climate forecasts. *Progress in Oceanography, 27*(2), 378-388.

Tommasi, D., Stock, C. A., Pegion, K., Vecchi, G. A., Methot, R. D., Alexander, M. A., & Checkley, D. M. (2017). Improved management of small pelagic fisheries through seasonal climate prediction. *Ecological Applications, 27*(2), 378-388.

Watelet, S. (2019). Gulf Stream indexes. from http://labos.ulg.ac.be/gher/home/people/sylvain-watelet/

Watelet, S., Beckers, J.-M., & Barth, A. (2017). Reconstruction of the Gulf Stream from 1940 to the Present and Correlation with the North Atlantic Oscillation. *Journal of Physical Oceanography, 47*(11), 2741-2754. doi: 10.1175/jpo-d-17-0064.1

Wood, R. J., & Austin, H. M. (2009). Synchronous multidecadal fish recruitment patterns in Chesapeake Bay, USA. *Canadian Journal of Fisheries and Aquatic Sciences, 66*(3), 496-508.

Wood, S. (2006). *Generalized Additive Models: An Introduction with R*. New York Chapman and Hall/CRC.

Zuur, A., Ieno, E. N., Walker, N., Saveliev, A. A., & Smith, G. M. (2009). *Mixed effects models and extensions in ecology with R. 2nd Edition*: Springer Science & Business Media.

FIGURE AND TABLE LEGENDS

Figure 1. Map of the golden tilefish management boundary separating northern and southern stocks on the US East Coast and NMFS statistical areas used for commercial catch and effort reporting.

Figure 2. Partial dependence plots estimated based on the random forest for northern landings of golden tilefish. See Table 1 for description of environmental factor abbreviations. Covariate time lags are described in parentheses as time of estimate (t) minus lag in years (y) or months (m).

Figure 3. Estimated smoothing curves for the GAMM of northern landings of golden tilefish. The tick marks on the inner horizontal axis denote positions of the observations; the dashed lines correspond to confidence bounds of ± 2 standard errors. See Table 1 for description of environmental factor abbreviations. Covariate time lags are described in parentheses as time of estimate (t) minus lag in years (y).

Figure 4. Shapley–Owen decomposition of GAM coefficients of determination (R^2). See Table 1 for description of environmental factor abbreviations. Covariate time lags are described in parentheses as time of estimate (t) minus lag in years (y), months (m), or quarters (q).

Figure 5. Estimated smoothing curves for the GAMM of northern stock CPUE for golden tilefish. The tick marks on the inner horizontal axis denote positions of the observations; the dashed lines correspond to confidence bounds of ± 2 standard errors. See Table 1 for description of environmental factor abbreviations. Covariate time lags are described in parentheses as time of estimate (t) minus lag in years (y) or quarters (q).

Figure 6. Estimated smoothing curves for the GAMM of southern stock CPUE. The tick marks on the inner horizontal axis denote positions of the observations; the dashed lines correspond to confidence bounds of ± 2 standard errors. See Table 1 for description of environmental factor abbreviations. Covariate time lags are described in parentheses as time of estimate (t) minus lag in years (y) or months (m).

Table 1. Covariates explored (denoted with an X) and selected (denoted with "*") in random forests (RFs) and generalized additive mixed models (GAMMs) of golden tilefish landings and

catch-per-unit-effort (CPUE) for both northern and southern stocks. Covariate time lags are described in parentheses.

Table 2. Prediction mean absolute error (PMAE) and prediction root mean square error (PRMSE) in units of $\sqrt{tonne}$ for the northern golden tilefish landings models and $\sqrt{pounds/day}$ for northern and southern catch-per-unit-effort (CPUE) models. Testing set size was 26 (1959–1970 and 1987–2000) for northern landings, 74 (2011–2013) for northern CPUE, and 318 (2011–2017) for southern CPUE models.

TABLES

Table 1. Covariates explored (denoted with an X) and selected (denoted with "*") in random forests (RFs) and generalized additive mixed models (GAMMs) of golden tilefish landings and catch-per-unit-effort (CPUE) for both northern and southern stocks. Covariate time lags are described in parentheses.

		Northern landings			Northern CPUE			Southern CPUE		
			RF	GAMM		RF	GAMM		RF	GAMM
Name	Description	Full	Final	Final	Full	Final	Final	Full	Final	Final
NAO_DJF_st	Station-based index of the North Atlantic Oscillation, Dec–Feb (0–7 years)	X	* (3, 4 years)	* (3, 4 years)						
NAO_DJF_PC	Principle component-based index of the North Atlantic Oscillation, Dec–Feb (0–7 years)	X	* (4 years)		X	* (0–7 years)		X	* (0–6 years)	
NAO_DJFMA_st	Station-based index of the North Atlantic Oscillation, Dec–Apr (0–7 years)	X								
NAO_DJFMA_PC	Principle component-based index of the North Atlantic Oscillation, Dec–Apr (0–7 years)	X			X	* (0–7 years)		X	* (0–7 years)	
AMO_annual	Annual Atlantic Multidecadal Oscillation index (0–7 years)	X	* (5–7 years)		X	* (0–7 years)	* (6 years)	X	* (0–7 years)	* (2, 4 years)
AMO_DJFMA	Atlantic Multidecadal Oscillation index, Dec–Apr (0–7 yrs)	X	* (5–7 years)	* (7 years)	X	* (0–7 years)	* (7 years)	X	* (0–7 years)	* (7 years)
Track_NE191	Index of Labrador Current surface (200 m) volume transport at OPEX/Poseidon-Jason Track NE191 (0–12 quarters)				X	* (0,4,9,10 quarters)	* (0 quarters)			
Track_226	Quarterly index of Labrador Current surface (200 m) volume transport at OPEX/Poseidon-Jason Track 226 (0–12 quarters)				X					

Table 1(cont'd).

Name	Description	Northern landings Full	Northern landings RF Final	Northern landings GAMM Final	Northern CPUE Full	Northern CPUE RF Final	Northern CPUE GAMM Final	Southern CPUE Full	Southern CPUE RF Final	Southern CPUE GAMM Final
Track_48	Quarterly index of Labrador Current surface (200 m) volume transport at OPEX/Poseidon-Jason Track 48 (0–12 quarters)				X					
Track_SW191	Quarterly index of Labrador Current surface (200 m) volume transport at OPEX/Poseidon-Jason Track SW191 (0–12 quarters)				X					
GSI	Quarterly index of anomalies in Gulf Stream position (0–12 quarters)				X	* (0,1,4–10,12 quarters)	* (12 quarters)			
GSNW	Annual index of Gulf Stream position along the north wall (0–3 years)				X	* (0–3 years)				
GSD	Annual index of Gulf Stream transport along the north wall (0–3 years)				X	* (0–3 years)				
FC_Transport	Monthly index of daily mean transport in the Florida Current (0–12 months)							X	* (0–12 months)	* (2–4,7,11 months)
avgP	Average monthly sea level pressure				X			X	*	
avgSST	Average monthly sea surface temperature				X			X	*	*
avgU	Average monthlyvector wind northward component				X			X	*	
avgV	Average monthly vector wind eastward component				X			X	*	
avgW	Average monthly scalar wind				X			X	*	
BTMPanom	Annual index of bottom temperature anomalies in the Mid-Atlantic Bight (0–7 years)				X	* (0–2,4–7 years)				
Time_block	Management/fishery time block	X	*		X	*		X	*	*
Area	NMFs statistical reporting area				X					
AREA_CENT_LAT	Centroid latitude of Area							X	*	*
AREA_CENT_LON	Centroid longitude of Area							X	*	
Month	Month				X			X	*	

Table 2. Prediction mean absolute error (PMAE) and prediction root mean square error (PRMSE) in units of $\sqrt{tonne}$ for the northern golden tilefish landings models and $\sqrt{pounds/day}$ for northern and southern catch-per-unit-effort (CPUE) models. Testing set size was 26 (1959–1970 and 1987–2000) for northern landings, 74 (2011–2013) for northern CPUE, and 318 (2011–2017) for southern CPUE models.

Model	Northern Landings		Northern CPUE		Southern CPUE	
	PMAE	PRMSE	PMAE	PRMSE	PMAE	PRMSE
RF	8.18	10.50	**5.91**	**7.16**	8.70	10.40
GAMM	**6.68**	**8.36**	6.22	7.60	**7.62**	**9.62**
GAM (GAMM without random effects)	7.82	9.85	6.66	7.86	8.06	10.20

FIGURES

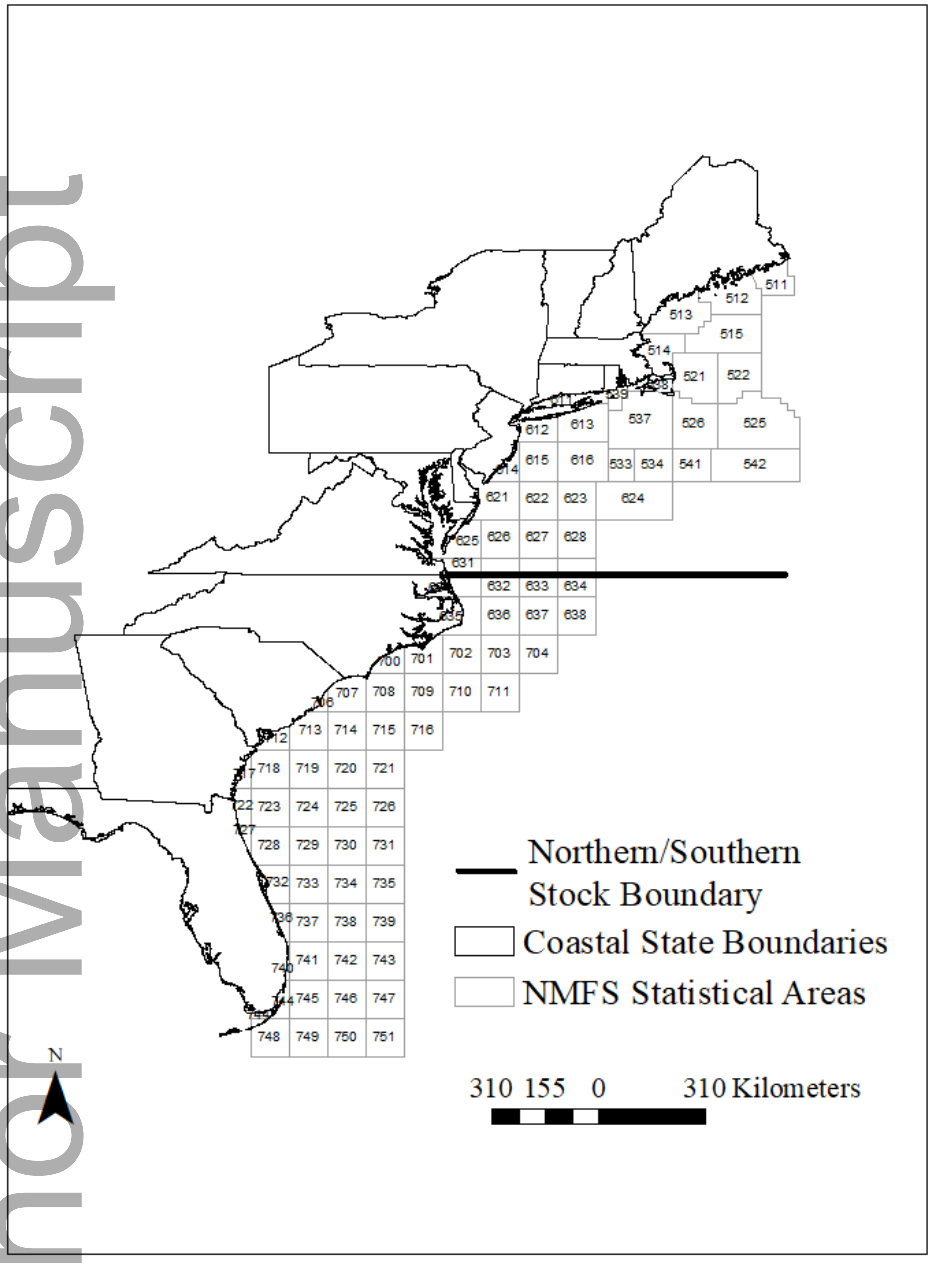

Figure 1. Map of the golden tilefish management boundary separating northern and southern stocks on the US East Coast and NMFS statistical areas used for commercial catch and effort reporting.

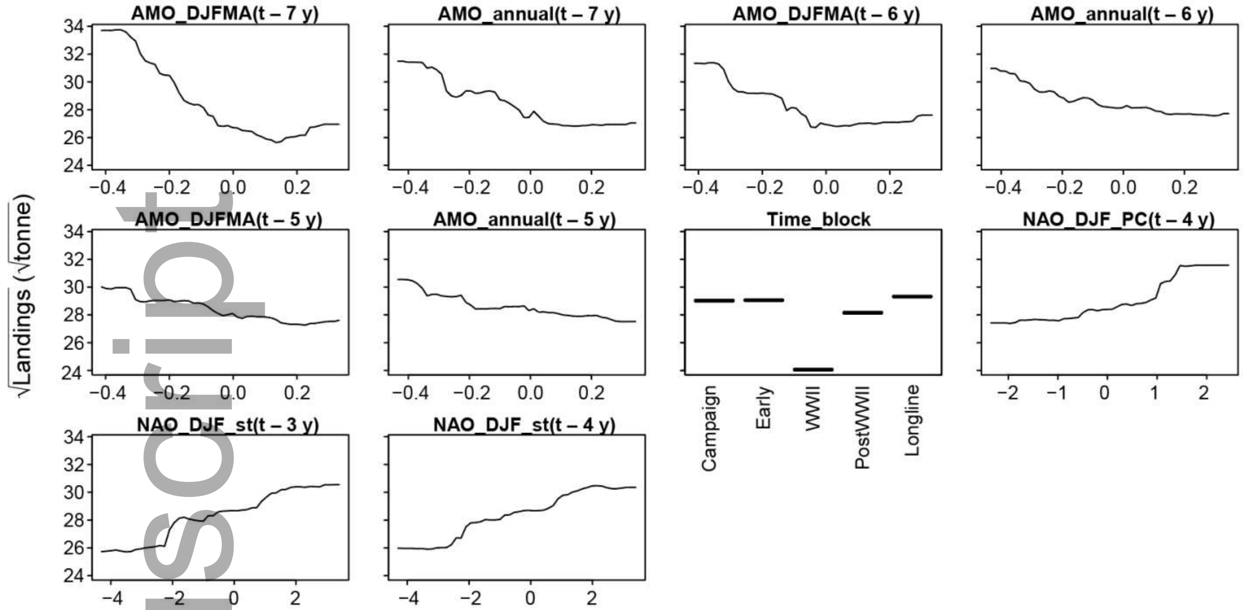

Figure 2. Partial dependence plots estimated based on the random forest for northern landings of golden tilefish. See Table 1 for description of environmental factor abbreviations. Covariate time lags are described in parentheses as time of estimate (t) minus lag in years (y) or months (m).

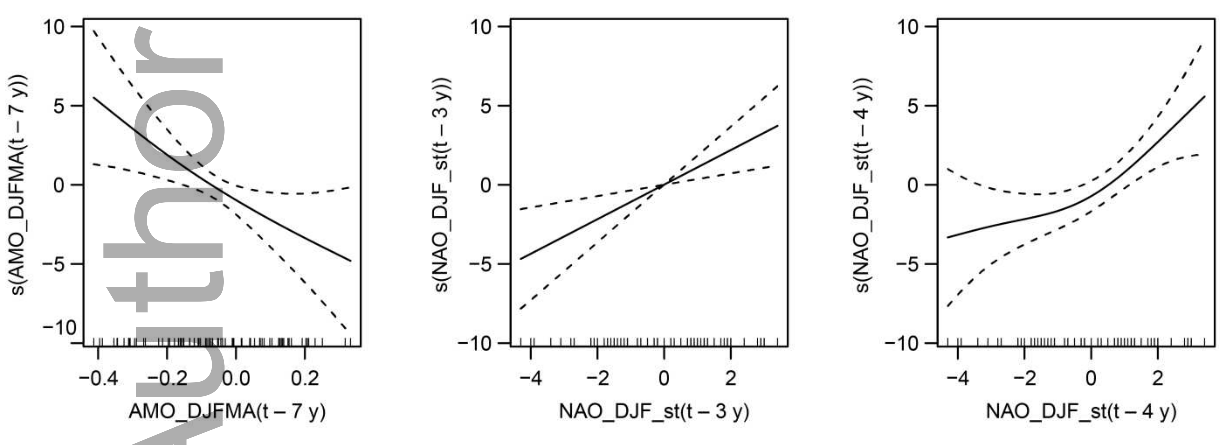

Figure 3. Estimated smoothing curves, s, for the GAMM of northern landings of golden tilefish. The curves are centered at 0; the dashed lines correspond to confidence bounds of ± 2 standard errors. The tick marks on the inner horizontal axis denote observed values of the covariates. See

Table 1 for description of environmental factor abbreviations. Covariate time lags are described in parentheses as time of estimate (t) minus lag in years (y).

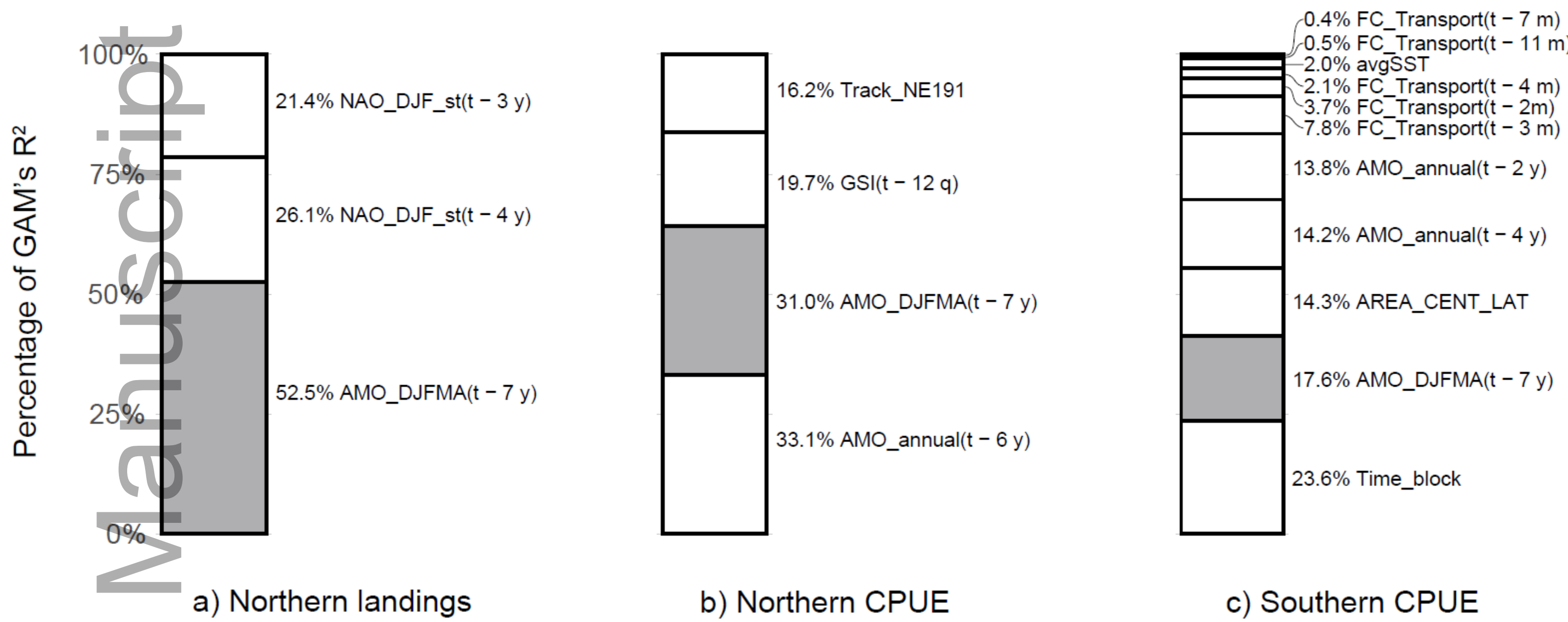

Figure 4. Shapley–Owen decomposition of GAM coefficients of determination (R^2). Gray shading highlights one variable shared by all three models, namely December to April AMO with a 7-year time lag. See Table 1 for description of environmental factor abbreviations. Covariate time lags are described in parentheses as time of estimate (t) minus lag in years (y), months (m), or quarters (q).

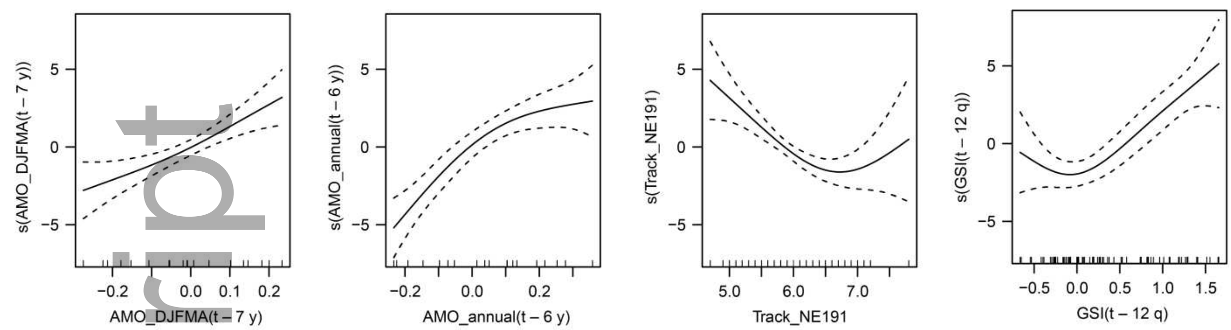

Figure 5. Estimated smoothing curves, s, for the GAMM of northern stock CPUE for golden tilefish. The curves are centered at 0; the dashed lines correspond to confidence bounds of ± 2 standard errors. The tick marks on the inner horizontal axis denote observed values of the covariates. See Table 1 for description of environmental factor abbreviations. Covariate time lags are described in parentheses as time of estimate (t) minus lag in years (y) or quarters (q).

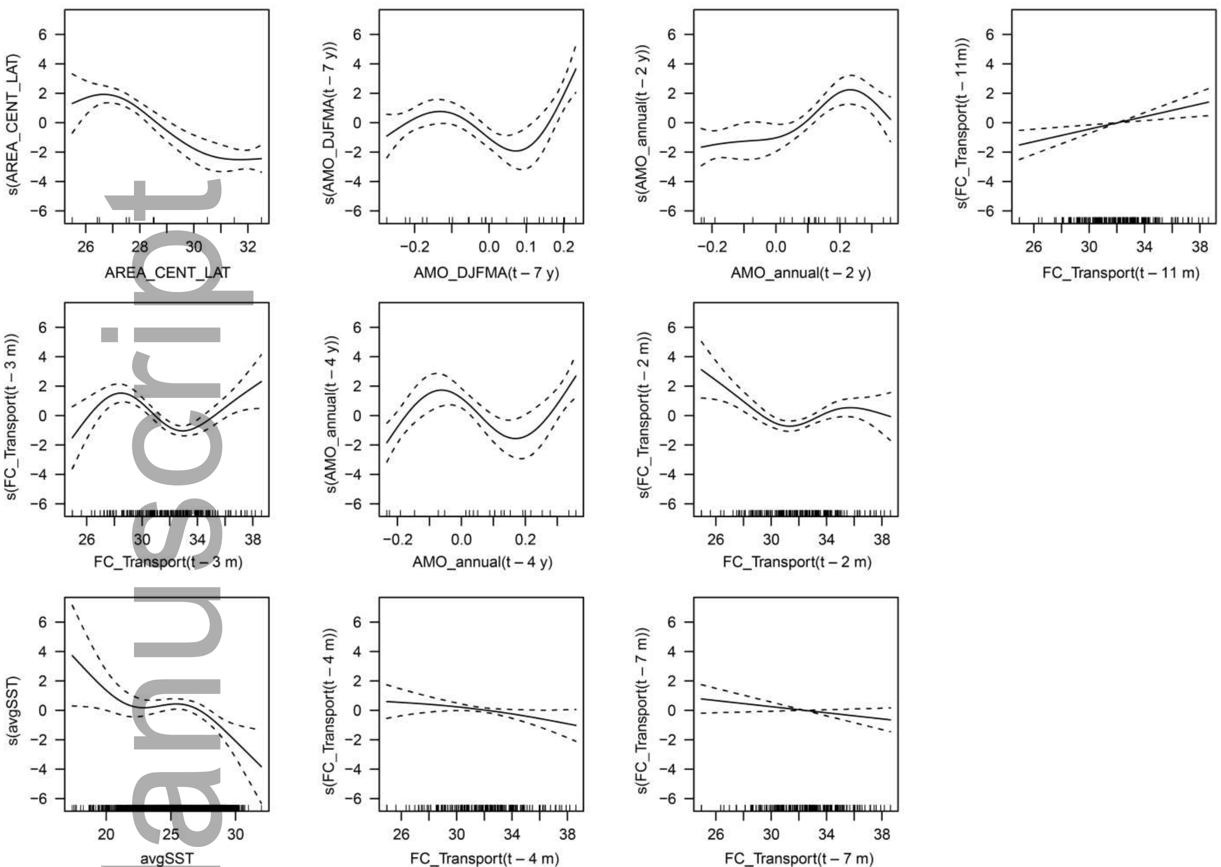

Figure 6. Estimated smoothing curves, s, for the GAMM of southern stock CPUE. The curves are centered at 0; the dashed lines correspond to confidence bounds of ± 2 standard errors. The tick marks on the inner horizontal axis denote observed values of the covariates. The estimated coefficient for categorical variable Time_block (pre-closures) is –6.679 (standard error 0.979). See Table 1 for description of environmental factor abbreviations. Covariate time lags are described in parentheses as time of estimate (t) minus lag in years (y) or months (m).

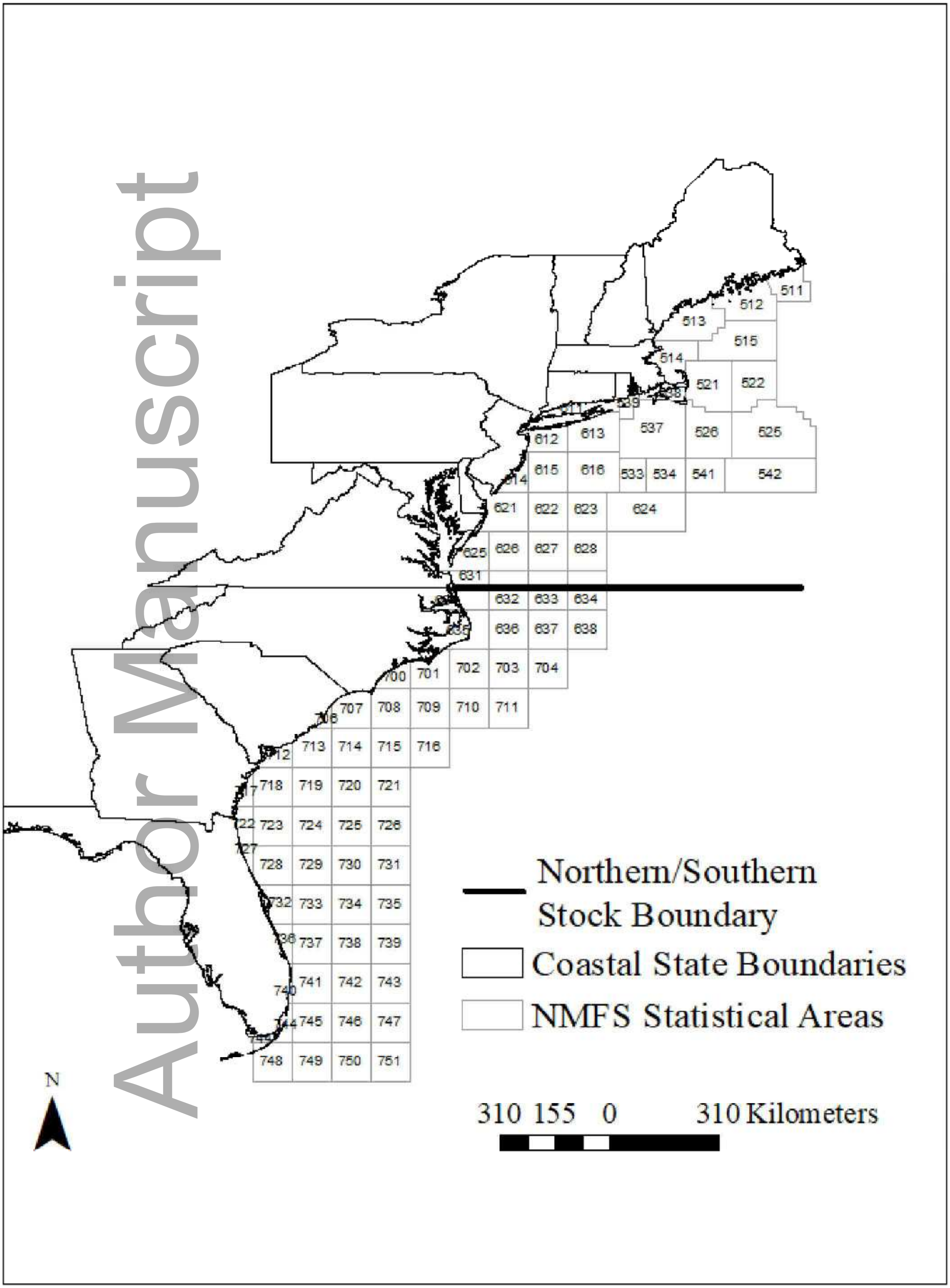
Northern/Southern
Stock Boundary
Coastal State Boundaries
NMFS Statistical Areas
310 155 0 310 Kilometers
N

fog_12540_f2.pdf

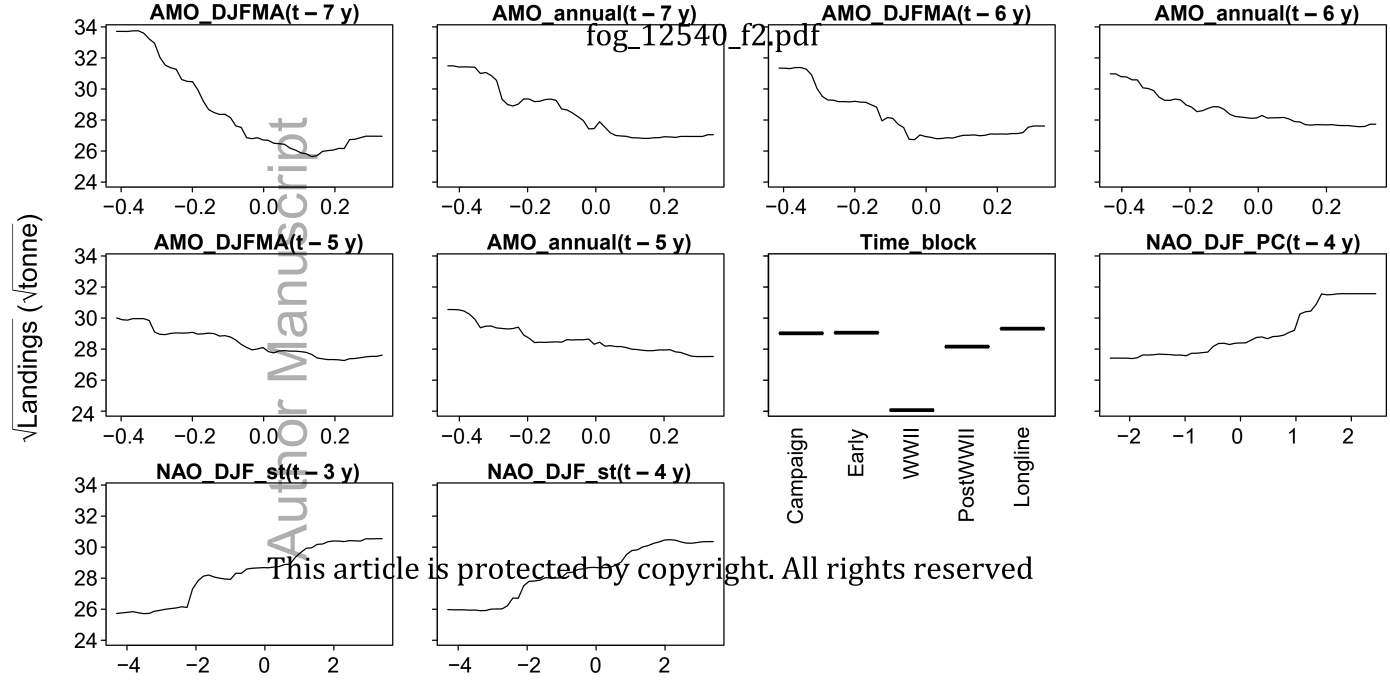

fog_12540_f3.pdf

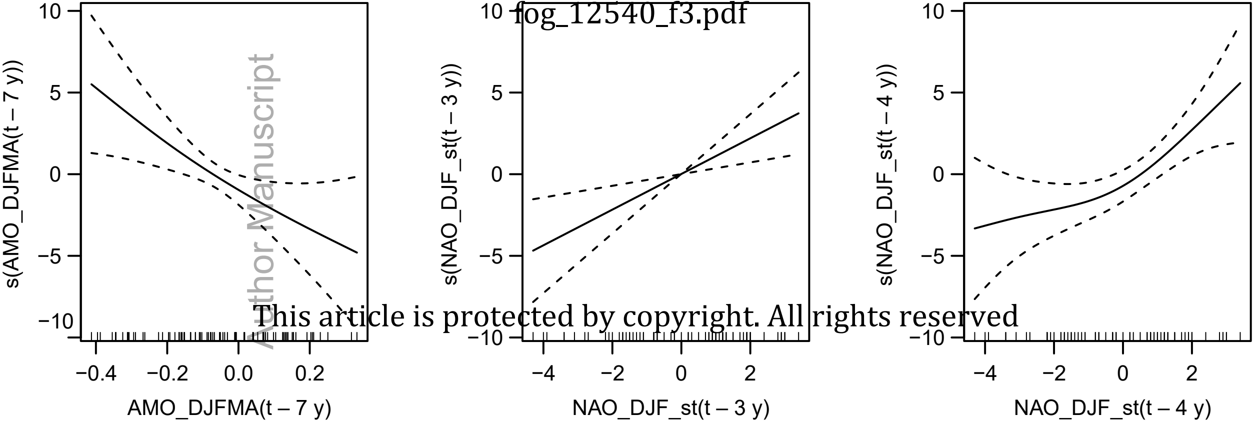

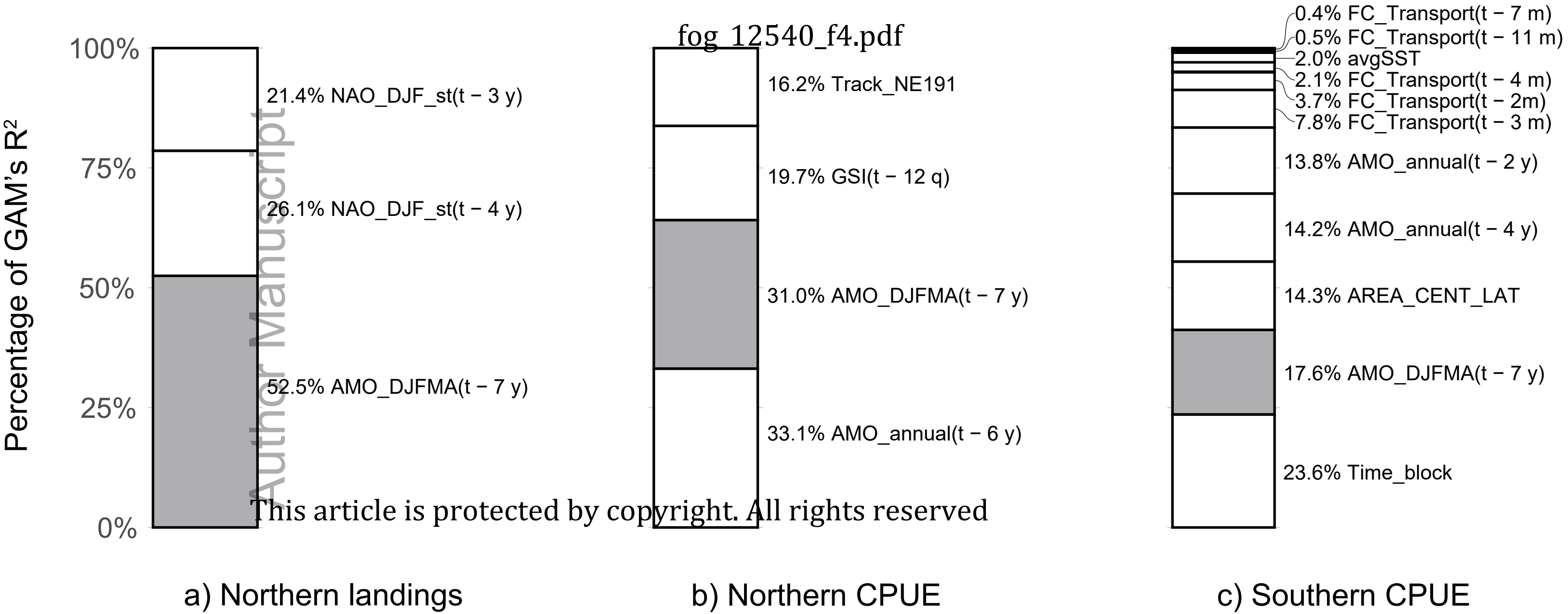
Percentage of GAM's R^2
100%
75%
50%
25%
0%
21.4% NAO_DJF_st(t − 3 y)
26.1% NAO_DJF_st(t − 4 y)
52.5% AMO_DJFMA(t − 7 y)
16.2% Track_NE191
19.7% GSI(t − 12 q)
31.0% AMO_DJFMA(t − 7 y)
33.1% AMO_annual(t − 6 y)
0.4% FC_Transport(t − 7 m)
0.5% FC_Transport(t − 11 m)
2.0% avgSST
2.1% FC_Transport(t − 4 m)
3.7% FC_Transport(t − 2m)
7.8% FC_Transport(t − 3 m)
13.8% AMO_annual(t − 2 y)
14.2% AMO_annual(t − 4 y)
14.3% AREA_CENT_LAT
17.6% AMO_DJFMA(t − 7 y)
23.6% Time_block
a) Northern landings
b) Northern CPUE
c) Southern CPUE

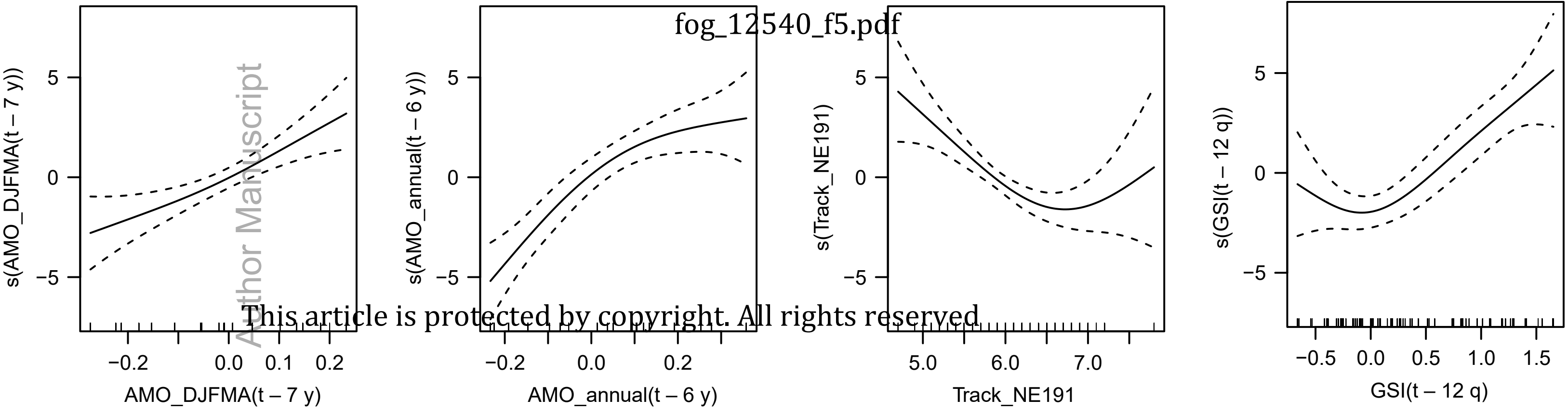
s(AMO_DJFMA(t – 7 y))
AMO_DJFMA(t – 7 y)
s(AMO_annual(t – 6 y))
AMO_annual(t – 6 y)
s(Track_NE191)
Track_NE191
s(GSI(t – 12 q))
GSI(t – 12 q)